Available online at www.sciencedirect.com
ScienceDirect
Ceramics International 34 (2008) 615–619
CERAMICS INTERNATIONAL
www.elsevier.com/locate/ceramint

Simultaneous pulsed current activated combustion synthesis and densification of $NbSi_2$–SiC composite

In-Jin Shon [a,*], Hyun-Kuk Park [a], Hwan-Cheol Kim [a], Jin-Kook Yoon [b], In-Yong Ko [a]

[a] School of Advanced Materials Engineering and Research Center for Advanced Materials Development, Engineering College, Chonbuk National University, 664-14 Deokjin-dong 1-ga, Deokjin-gu, Jeonju, Jeonbuk 561-756, South Korea
[b] Metal Processing Research Center, Korea Institute of Science and Technology, P.O. Box 131, Cheongryang, Seoul 136-791, South Korea

Received 25 September 2006; received in revised form 4 November 2006; accepted 22 December 2006
Available online 2 February 2007

Abstract

Dense ultrafine $NbSi_2$–SiC composite was synthesized by the pulsed current activated combustion synthesis (PCACS) method within 3 min in one step from mechanically activated powders of NbC and 3Si. Simultaneous combustion synthesis and densification were accomplished under the combined effects of a pulsed current and mechanical pressure. Highly dense $NbSi_2$–SiC composite with relative density of up to 97% was produced under simultaneous application of a 60 MPa pressure and the electric current. The average grain size and mechanical properties (hardness and fracture toughness) of the composite were investigated.

Keywords: A. Sintering; C. Mechanical properties; Pulsed current activated combustion; Composite materials; Intermetallic; Nanophase; $NbSi_2$–SiC

1. Introduction

Interest in refractory metal silicides has increased significantly in recent years because of their potential application as high-temperature structural materials [1]. This class of materials has an attractive combination of properties, including high melting temperature, high modulus, high oxidation resistance in air, and a relatively low density [2,3]. However, as in the case of many intermetallic compounds, the current concern about these materials focuses on their low fracture toughness below the ductile-brittle transition temperature [4–6]. To improve on their mechanical properties, the approach commonly utilized has been the addition of a second phase to form composites [7–12]. An example is the addition of SiC to $NbSi_2$ to improve the latter's properties. SiC is a very interesting ceramic material due to its properties like high hardness, low bulk density and high oxidation resistance which made SiC useful for a wide range of industrial application. Furthermore, the isothermal oxidation resistance of metal silicide–SiC composite in dry air was superior to that of monolithic metal silicide compact [13]. Therefore, SiC may be the most promising additive as a reinforcing material for $NbSi_2$-based composites.

Many similar high-temperature dense composites are usually prepared in a multi-step process [14,15]. However, the method of field-activated and pressure-assisted combustion synthesis has been successfully employed to synthesize and densify materials from the elements in one step in a relatively short period of time. This method has been used to synthesize a variety of ceramics and composites, including $MoSi_2$–ZrO_2, Ti_5Si_3 and its composites, WSi_2 and its composites, and WC–Co hard materials [16–23]. These materials, which are generally characterized by low adiabatic combustion temperatures, cannot be synthesized directly by the self-propagating high-temperature synthesis (SHS) method. The objective of this study is to investigate the preparation of dense nanophase $NbSi_2$–SiC composite by the PCACS method starting from a mixture of mechanically activated NbC and 3Si powders. The interaction between these phases, i.e.,

$$NbC + 3Si \rightarrow NbSi_2 + SiC, \quad (1)$$

is thermodynamically feasible.

* Corresponding author.
E-mail address: ijshon@chonbuk.ac.kr (I.-J. Shon).

0272-8842/$34.00
doi:10.1016/j.ceramint.2006.12.012

2. Experimental procedure

Powders of 99.5% niobium carbide (−325 mesh, Cerac Products) and 99.5% pure silicon (−325 mesh, Alfa Products) were used as a starting materials. Fig. 1 shows SEM images of the raw materials used. Powder mixtures of NbC and Si in the molar proportion of 1:3 were first milled in a high-energy ball mill (Pulverisette-5, planetary mill) at 250 rpm for 10 h. Tungsten carbide balls (5 mm in diameter) were used in a sealed cylindrical stainless steel vial under argon atmosphere. The weight ratio of ball-to-powder was 30:1. Milling resulted in a significant reduction of grain size. The grain size and the internal strain were calculated by Stokes and Wilson's formula [22],

$$b = b_d + b_e = \frac{k\lambda}{d\cos\theta + 4\varepsilon\tan\theta} \quad (2)$$

where b is the full width at half-maximum (FWHM) of the diffraction peak after instrument correction; b_d and b_e the FWHM caused by small grain size and internal stress, respectively; k the constant (with a value of 0.9); λ the wavelength of the X-ray radiation; d and ε the grain size and internal stress, respectively; and θ is the Bragg angle. The parameters b and b_s follow Cauchy's form with the relationship: $B_0 = b + b_s$, where B_0 and b_s are FWHM of the broadened Bragg peaks and the standard sample's Bragg peaks, respectively. Fig. 2 shows XRD

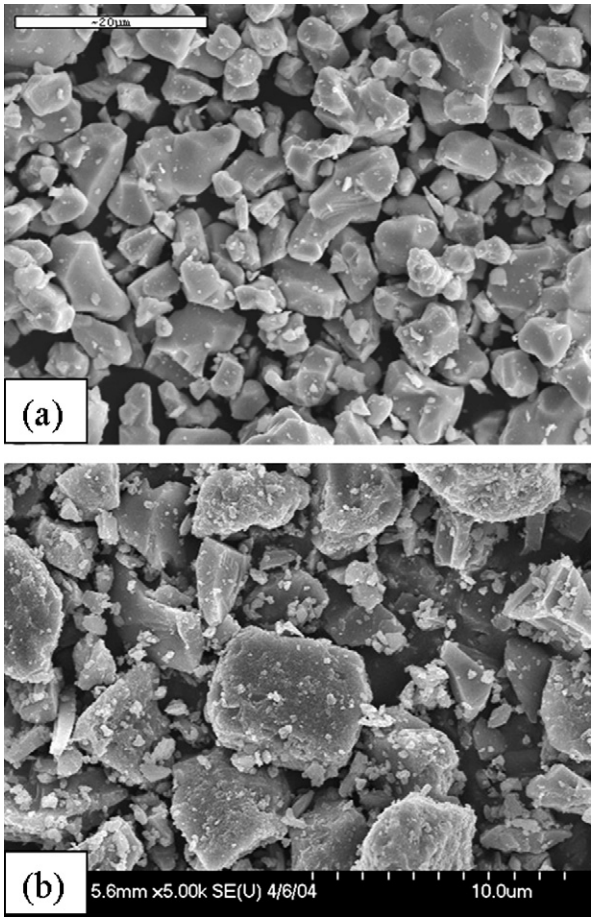

Fig. 1. Scanning election microscope images of raw materials: (a) niobium carbide and (b) silicon.

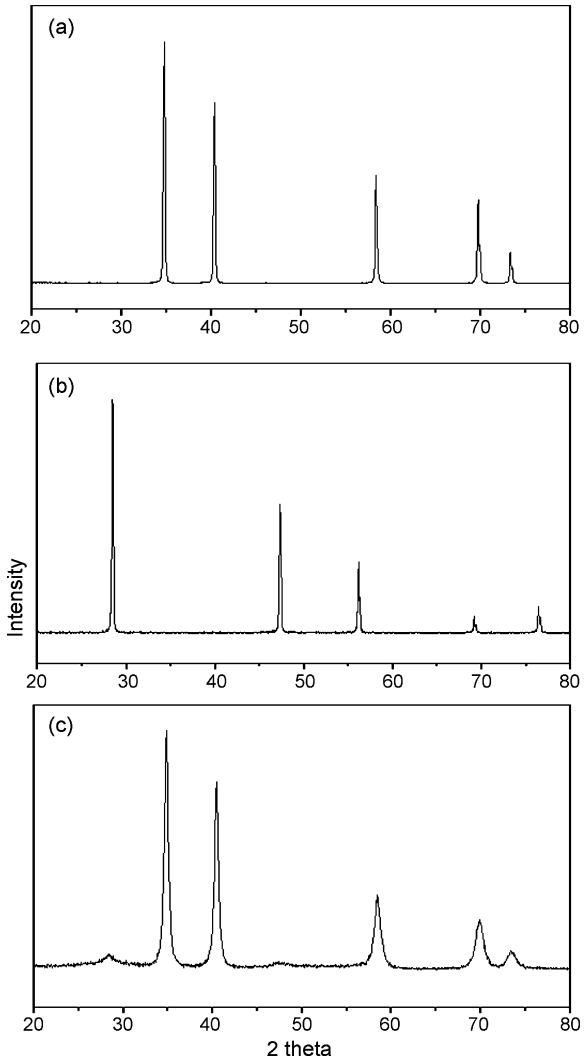

Fig. 2. XRD patterns of raw materials: (a) NbC, (b) Si and (c) milled NbC + 3Si.

patterns of the raw powders and the milled NbC + 3Si powder mixture. The FWHM of the milled powder is greater than that of the raw powders due to internal strain and grain size reduction. The average grain sizes of the milled NbC and Si powders were determined as 89 and 26 nm, respectively.

After milling, the mixed powders were placed in a graphite die (outside diameter, 45 mm; inside diameter, 20 mm; height, 40 mm) and then introduced into the pulsed-current activated sintering system made by Eltek Co. in Republic of Korea. Schematic diagram of this method is shown in Fig. 3. The PCACS apparatus includes an 18 V, 2800 A dc power supply (which provides a pulsed current with 20 s on time and 10 s off time through the sample and die) and a 50 kN uniaxial press. The system was first evacuated and a uniaxial pressure of 60 MPa was applied. A pulsed dc current was then activated and maintained until the densification rate was negligible, as indicating by the observed shrinkage of the sample. Sample shrinkage is measured in real time by a linear gauge measuring the vertical displacement. Temperatures were measured by a pyrometer focused on the surface of the graphite die. Depending on heating rate, the electrical and thermal

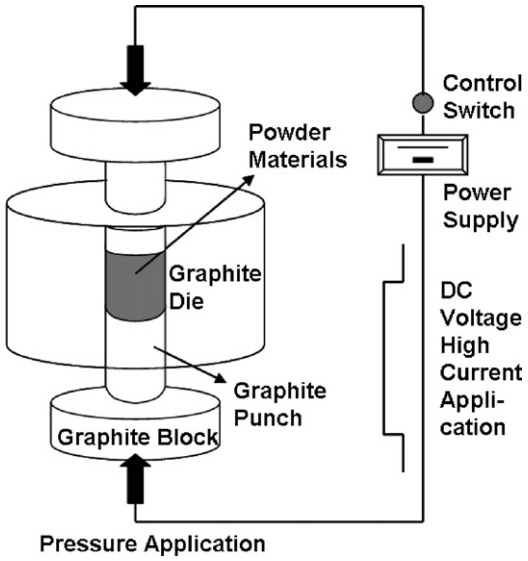

Fig. 3. Schematic diagram of the pulsed current activated combustion apparatus.

conductivities of the compact, and on its relative density, a difference in temperature between the surface and the center of the sample exists. At the end of the process, the current was turned off and the sample was allowed to cool to room temperature. The entire process of densification using the PCACS technique consists of four major control stages. These are chamber evacuation, pressure application, power application, and cool down. The process was carried out under a vacuum of 40 mTorr.

The relative densities of the synthesized sample were measured by the Archimedes method. Microstructural characterization was made on product samples which had been polished and etched using a solution of HF (30 vol.%), HNO_3 (30 vol.%) and H_2O (40 vol.%) for 10 s at room temperature. Compositional and microstructural analyses of the products were made through X-ray diffraction (XRD) and scanning electron microscopy (SEM) with energy dispersive X-ray analysis (EDAX). Vickers hardness was measured by performing indentations at a load of 10 kg and a dwell time of 15 s.

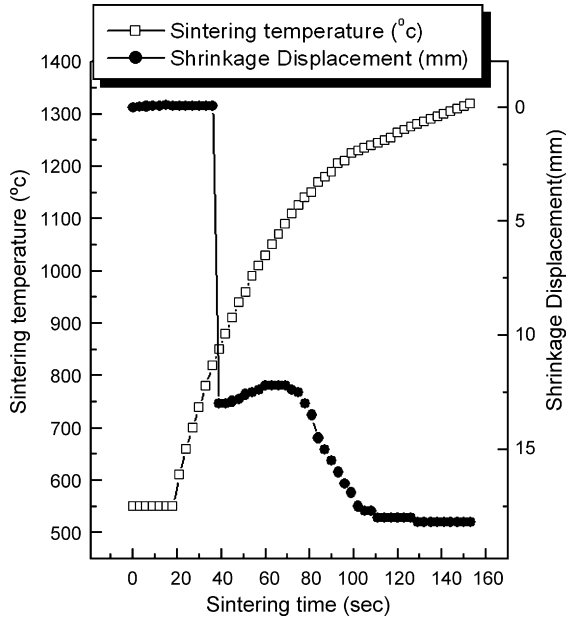

Fig. 4. Variations of temperature and shrinkage displacement with heating time during pulsed current activated combustion synthesis and densification of $NbSi_2$–SiC composite (under 60 MPa, 2800 A).

3. Results and discussion

The variations in shrinkage displacement and temperature with heating time during the processing of NbC + 3Si system

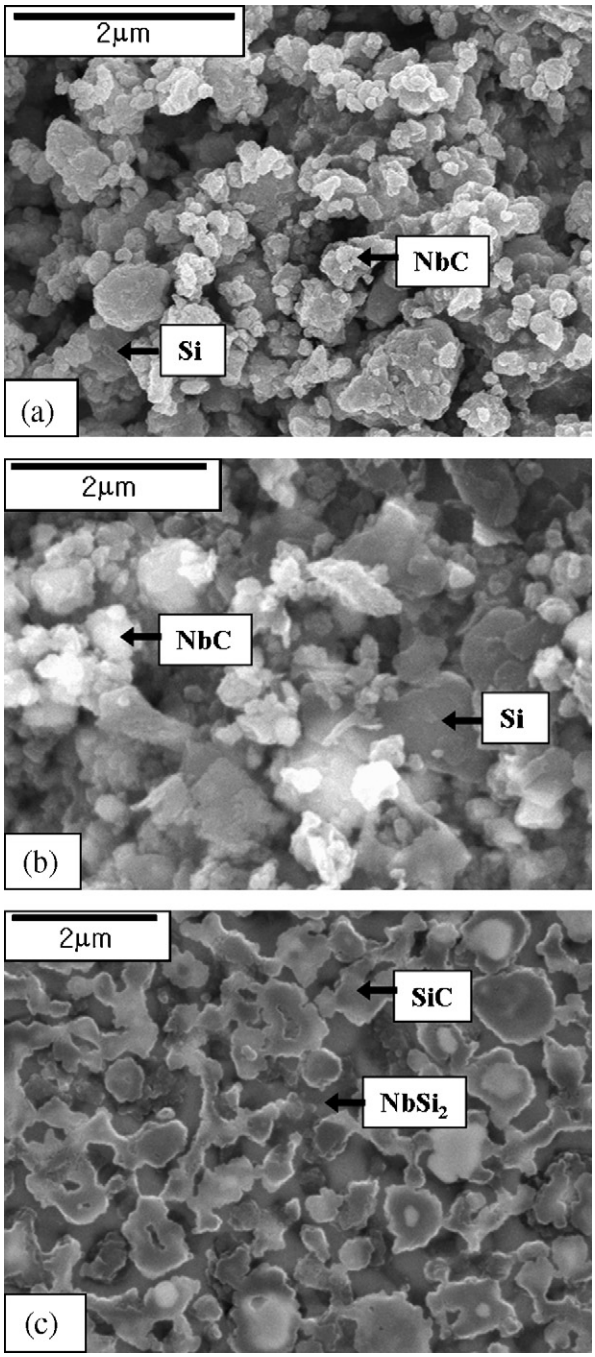

Fig. 5. Scanning electron microscope images of NbC + 3Si system: (a) after milling, (b) before combustion synthesis, and (c) after combustion synthesis.

are shown in Fig. 4. As the pulsed current was applied the specimen showed initially a small (thermal) expansion and then increased abruptly at approximately 850 °C. When the reactant mixture of NbC + 3Si was heated under 60 MPa pressure to 800 °C, no reaction took place and no significant shrinkage displacement as judged by subsequent XRD and SEM analyses. Fig. 5(a)–(c) shows the SEM (secondary electron) images of (a) powder after milling, (b) sample heated to 800 °C and (c) sample heated to 1300 °C, respectively. Fig. 6(a) and (b) shows the presence of the reactants as separate phases. X-ray diffraction results, shown in Fig. 6(a) and (b) exhibit only peaks pertaining to the reactants NbC and Si. However, when the temperature was raised to 1300 °C, the starting powders reacted producing highly dense products. SEM image of the etched surfaces of the samples heated to 1300 °C under a pressure of 60 MPa is shown in Fig. 5(c). A complete reaction between NbC and Si took place under these conditions. These conclusions were supported by X-ray diffraction analyses with peaks of the product phase, $NbSi_2$ and SiC phase, as indicated in Fig. 6(c). Furthermore, a minor phase (Nb_5Si_3) observed by X-ray diffraction analyses, as show in Fig. 6(c). The presence of Nb_5Si_3 in the sample suggests a deficiency of Si. It is considered that this observation is related to entrapped oxygen in the pores of the interior portion of the sample during pressing and to a little amount of oxidation of Si during the heating. The abrupt increase in the shrinkage displacement at the ignition temperature is due to the increase in density as a result of molar volume change associated with the formation of $NbSi_2$–SiC from the reactants (NbC and Si) and the consolidation of the product. It should be recalled that the measured temperatures are those of the surface of the die and are, therefore, likely to be different than the values in the middle of the sample. Thus, the onset of the reaction to form the composite (and the concomitant rapid shrinkage) may be at a higher temperature than the observed value of 850 °C.

Dependence of relative densities and crystallite size of $NbSi_2$ with heating temperature are shown in Fig. 7. As can be expected, the relative densities and grain size rapidly increase

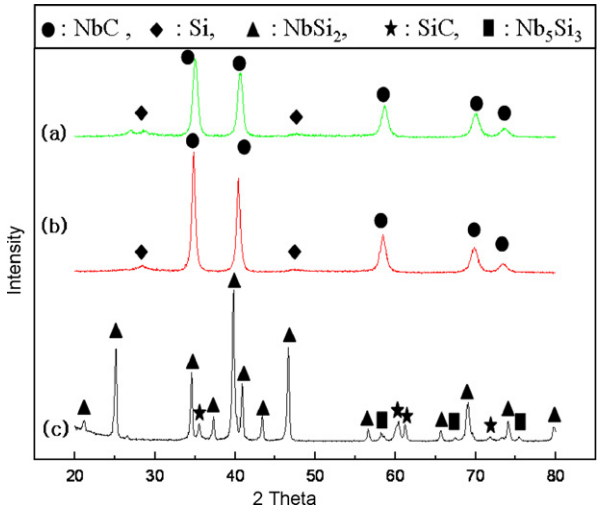

Fig. 6. XRD patterns of the NbC + 3Si system: (a) after milling, (b) before combustion synthesis, and (c) after combustion synthesis.

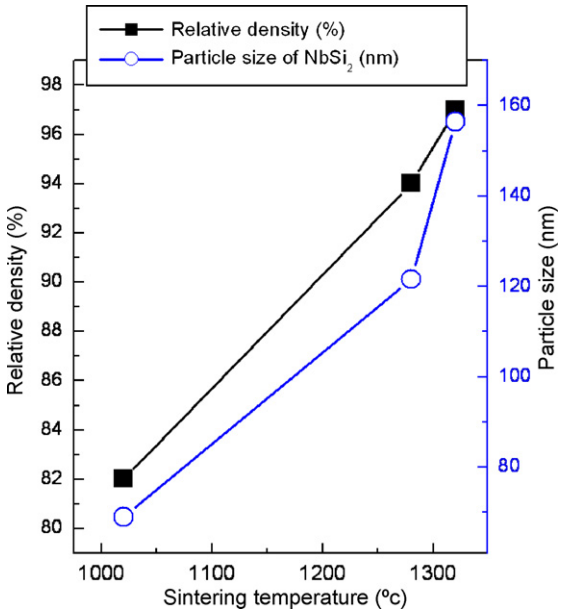

Fig. 7. Variation of relative density and crystallite size of $NbSi_2$ with heating temperature without holding time under pressure of 60 MPa.

with heating temperature from 82 to 97% and from 70 to 157 nm, respectively. The SiC particles were well distributed in matrix, as can bee seen from the SEM image, Fig. 5(c).

Vickers hardness measurements were made on polished sections of the $NbSi_2$–SiC composite using a 10 kg_f load and 15 s dwell time. The calculated hardness value, based on an average of five measurements, of the $NbSi_2$–SiC composite is 1260 kg/mm^2. Indentations with large enough loads produced median cracks around the indent. The length of these cracks permits an estimation of the fracture toughness of the materials by means of the expression [23]:

$$K_{IC} = 0.204\left(\frac{c}{a}\right)^{-3/2} H_v a^{1/2} \quad (3)$$

where c is the trace length of the crack measured from the center of the indentation, a is half of the average length of two indent diagonals and H_v is the hardness. A typical indentation pattern for the $NbSi_2$–SiC composite is shown in Fig. 8(a). Typically, one to three additional cracks were observed to propagate from the indentation corner. The calculated fracture toughness value for the $NbSi_2$–SiC composite is approximately 5.3 MPa $m^{1/2}$ As in the case of the hardness value, the toughness values are an average of five measurements. A higher magnification view of the indentation median crack in the composite is shown in Fig. 8(b). This shows the crack propagates along phase boundary of $NbSi_2$ and SiC.

The absence of reported values for hardness and toughness on $NbSi_2$–SiC precludes making direct comparison to the results obtained in this work to show the influence of grain size. Similarly, an absence of corresponding data on $NbSi_2$ makes it difficult to show the effect of the addition of SiC. The only related study reported in the literature that we are cognizant of is that by Guille and Matini [24]. The investigated the

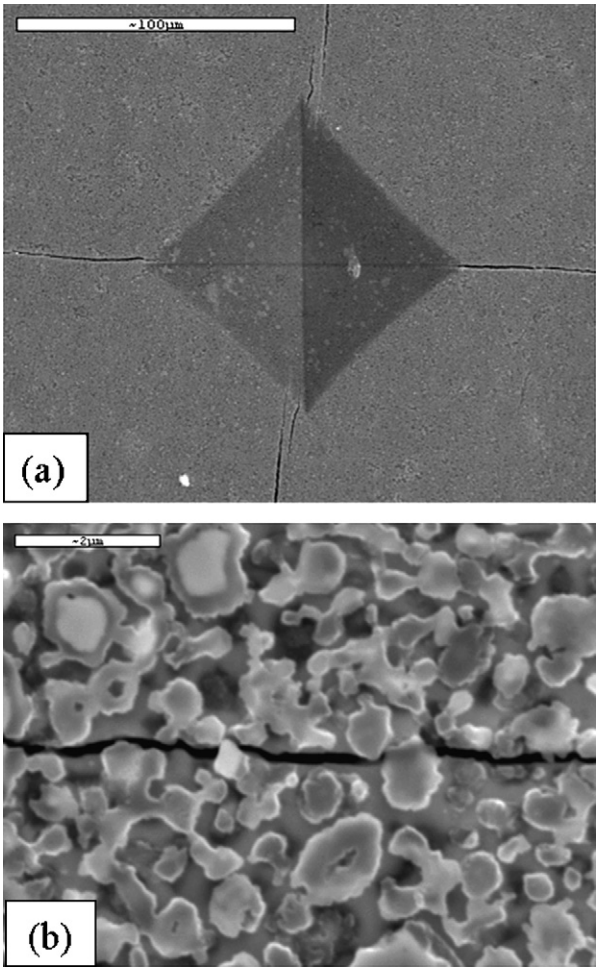

Fig. 8. (a) Vickers hardness indentation and (b) median crack propagating of $NbSi_2$–SiC composite.

microhardness and fracture toughness of silicide coatings on metal substrates. Coatings of thicknesses ranging from 30 to 40 μm were formed. In the case of Nb substrates, the coating was composed of a layer $NbSi_2$ only. It was found that the hardness of $NbSi_2$ depended on the applied load, being constant, at a value of about 10 GPa, in the load range of 0.15–0.6 N, but increased linearly at higher loads. The calculated fracture toughness, however, was independent of load, being about 2 MPa $m^{1/2}$. Although a direct comparison cannot be made, but the hardness of our composite is higher than the lowest value 10 GPa at 0.15–0.6 N in the reported literature account results. Likewise, the fracture toughness in the composite of this work (5.3 MPa $m^{1/2}$) is more than 100% higher than the value in the cited reference [24].

4. Summary

Using the pulsed current activated combustion method, the simultaneous synthesis and densification of ultrafine $NbSi_2$–SiC composite was accomplished using powders of NbC and 3Si. Complete synthesis and densification can be achieved in one step within 3 min. The relative density of the composite was 97% under an applied pressure of 60 MPa and the pulsed current. The average grain sizes of $NbSi_2$ phases in the composite were approximately 157 nm. The average hardness and fracture toughness values obtained were 1260 kg/mm^2 and 5.3 MPa $m^{1/2}$, respectively. The lack of reported data on $NbSi_2$–SiC makes difficult to make direct comparisons, but based on reported data on $NbSi_2$ coating, an approximate comparison shows that the present results exhibit a higher hardness and toughness.

Acknowledgments

We are grateful for the financial support from the Korea Institute of Science and Technology, which was provided through the program for study on Technologies for Formation and Evaluation of Nano-Structured Composite Coatings.

References

[1] N.S. Stoloff, J. Mater. Sci. Eng. A261 (1999) 169–180.
[2] A.K. Vasudevan, J.J. Petrovic, J. Mater. Sci. Eng. A155 (1992) 259–266.
[3] G.J. Fan, M.X. Quan, Z.Q. Hu, J. Eckert, L. Schulz, Scripta Mater. 41 (1999) 1147–1151.
[4] G. Sauthoff, Intermetallics, VCH Publishers, New York, 1995.
[5] Y. Ohya, M.J. Hoffmann, G. Petzow, J. Mater. Sci. Lett. 12 (1993) 149–152.
[6] J. Qian, L.L. Daemen, Y. Zhao, Diamond Relat. Mater. 14 (2005) 1669–1672.
[7] B.W. Lin, T. Iseki, Br. Ceram. Trans. J. 91 (1992) 1–5.
[8] Y. Ohya, M.J. Hoffmann, G. Petzow, J. Am. Ceram. Soc. 75 (1992) 2479–2483.
[9] S.K. Bhaumik, C. Divakar, A.K. Singh, G.S. Upadhyaya, J. Mater. Sci. Eng. A 279 (2000) 275–281.
[10] D.K. Jang, R. Abbaschian, Kor. J. Mater. Res. 9 (1999) 92–98.
[11] H. Zhang, P. Chen, M. Wang, X. Liu, Rare Metals 21 (2002) 304–307.
[12] D.Y. Oh, H.C. Kim, J.K. Yoon, I.J. Shon, J. Alloys Compnds. 395 (2005) 174–180.
[13] J.k. Yoon, K.H. Lee, G.H. Kim, J.H. Han, J.M. Doh, K.T. Hong, Mater. Trans. 45 (7) (2004) 2435–2442.
[14] K. Bhattacharya, J.J. Petrovic, J. Am. Ceram. Soc. 74 (1991) 2700–2703.
[15] Y. Luo, S. Li, W. Pan, L. Li, Mater. Lett. 58 (2003) 150–153.
[16] Z.A. Munir, I.J. Shon, K. Yamazaki, U.S. Patent No. 5,794,113 (1998)
[17] I.J. Shon, Z.A. Munir, K. Yamazaki, K. Shoda, J. Am. Ceram. Soc. 79 (1996) 1875–1880.
[18] I.J. Shon, H.C. Kim, D.H. Rho, Z.A. Munir, Mater. Sci. Eng. A 269 (1999) 129–135.
[19] I.J. Shon, D.H. Rho, H.C. Kim, Z.A. Munir, J. Alloys Compnds. 322 (2001) 120–126.
[20] I.J. Shon, D.H. Rho, H.C. Kim, Met Mater. 6 (2000) 533–541.
[21] C.D. Park, H.C. Kim, I.J. Shon, Z.A. Munir, J. Am. Ceram. Soc. 85 (2002) 2670–2677.
[22] F.L. Zhang, C.Y. Wang, M. Zhu, Scripta Mater. 49 (2003) 1123–1128.
[23] K. Niihara, Ceramics 20 (1985) 1218–1224.
[24] J. Guille, L. Matini, J. Mater. Sci. Lett. 7 (1988) 952–954.